AD-A077 880 ARMY ELECTRONICS RESEARCH AND DEVELOPMENT COMMAND WS--ETC F/G 4/1
VALIDATION OF THE DAIRCHEM CODE I: QUIET MIDLATITUDE CONDITIONS--ETC(U)
SEP 79 M G HEAPS , J M HEIMERL

UNCLASSIFIED ERADCOM/ASL-TR-0041 NL

1 OF 1
ADA 077880

END
DATE FILMED
1 -80
DDC

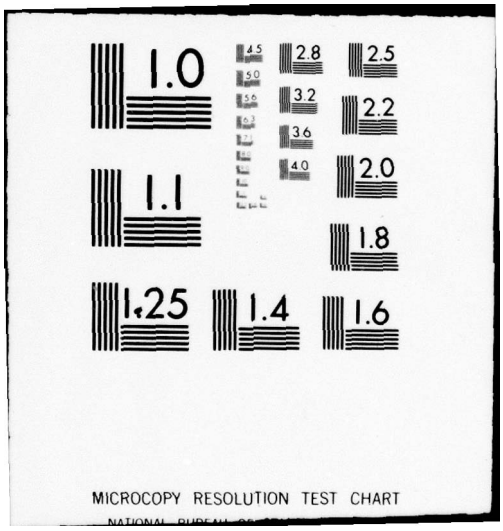
1.0
2.8
2.5
3.2
2.2
3.6
2.0
4.0
1.1
1.8
1.25
1.4
1.6
MICROCOPY RESOLUTION TEST CHART

(14) ERADCOM/ ASL-TR-0041

(12) 15

AD

Reports Control Symbol
OSD 1366

AD A077880

LEVEL II

(6) # VALIDATION OF THE DAIRCHEM CODE I: QUIET MIDLATITUDE CONDITIONS.

(9) Research and development rept.

(11) SEPTEMBER 1979

(12) 42

By

(10) MELVIN G. HEAPS

US Army Atmospheric Sciences Laboratory
White Sands Missile Range, New Mexico 88002

JOSEPH M. HEIMERL

US Army Ballistic Research Laboratory
Aberdeen Proving Ground, MD 21005

(16) 1L161102B53A (17) 12

Approved for public release; distribution unlimited

US Army Electronics Research and Development Command
ATMOSPHERIC SCIENCES LABORATORY
White Sands Missile Range, NM 88002

NOTICES

Disclaimers

The findings in this report are not to be construed as an official Department of the Army position, unless so designated by other authorized documents.

The citation of trade names and names of manufacturers in this report is not to be construed as official Government indorsement or approval of commercial products or services referenced herein.

Disposition

Destory this report when it is no longer needed. Do not return it to the originator.

SECURITY CLASSIFICATION OF THIS PAGE *(When Data Entered)*

REPORT DOCUMENTATION PAGE

READ INSTRUCTIONS BEFORE COMPLETING FORM

1. REPORT NUMBER: ASL-TR-0041	2. GOVT ACCESSION NO.
3. RECIPIENT'S CATALOG NUMBER	
4. TITLE *(and Subtitle)*: VALIDATION OF THE DAIRCHEM CODE I: QUIET MIDLATITUDE CONDITIONS	5. TYPE OF REPORT & PERIOD COVERED: R&D Technical Report
	6. PERFORMING ORG. REPORT NUMBER
7. AUTHOR(s): Melvin G. Heaps, ERADCOM, ASL, WSMR, NM 88002; Joseph M. Heimerl, BRL, Aberdeen Proving Ground, MD 21005	8. CONTRACT OR GRANT NUMBER(s)
9. PERFORMING ORGANIZATION NAME AND ADDRESS: Atmospheric Sciences Laboratory, White Sands Missile Range, NM 88002	10. PROGRAM ELEMENT, PROJECT, TASK AREA & WORK UNIT NUMBERS: DA Task No. 1L161102B53A-12
11. CONTROLLING OFFICE NAME AND ADDRESS: US Army Electronics Research and Development Command, Adelphi, MD 20783	12. REPORT DATE: September 1979
	13. NUMBER OF PAGES: 31
14. MONITORING AGENCY NAME & ADDRESS *(if different from Controlling Office)*	15. SECURITY CLASS. *(of this report)*: UNCLASSIFIED
	15a. DECLASSIFICATION/DOWNGRADING SCHEDULE

16. DISTRIBUTION STATEMENT *(of this Report)*

Approved for public release; distribution unlimited.

17. DISTRIBUTION STATEMENT *(of the abstract entered in Block 20, if different from Report)*

18. SUPPLEMENTARY NOTES

19. KEY WORDS *(Continue on reverse side if necessary and identify by block number)*

D region
Ion chemistry
Electron density
Positive ions
Negative ions
Ionospheric modeling

20. ABSTRACT *(Continue on reverse side if necessary and identify by block number)*

Two long-standing problems in the atmospheric sciences have been the correct modeling of the ion chemistry in the earth's atmosphere and the proper determination of the ion species and densities through in situ measurements. Comparison between experimental data and simultaions of those data by computer modeling of atmospheric chemistry is a means of validating the computer code as well as indicating which processes are in need of further study. The DAIRCHEM computer code is used here to simulate data taken in the midlatitude D region during quiet conditions. Comparison between the total positive ion

DD FORM 1 JAN 73 1473 EDITION OF 1 NOV 65 IS OBSOLETE

SECURITY CLASSIFICATION OF THIS PAGE *(When Data Entered)*

20. ABSTRACT (cont)

density profile derived from rocket measurements and the one computed by the code shows very good agreement in the 30 to 90 km range, with the exception that the simulated ion density profile is of somewhat smaller magnitude than the experimental one in the 60 and 75 km region. Such a discrepancy is only partially explained by the uncertainties in the ionization rate of NO due to Lyman alpha radiation. Comparison between the measured and the computed electron density profiles shows that the measured profile is consistently of a smaller magnitude than the computer profile in the 65 and 85 km range. We interpret this discrepancy as a deficiency in the modeling of the negative ion chemistry. Also, this deficiency is probably the main cause of the disparity between the total positive ion density profiles in the corresponding altitude range. The authors feel that the positive ion chemistry is reasonably well understood and that this section of the DAIRCHEM code may be considered validated. The negative ion chemistry needs to be studied further. Specifically, alternate electron attachment/detachment processes should be considered, as well as an as-yet-undetermined, possibly very massive, negative species which may affect the ion recombination rates. Successful modeling of the D region under naturally occurring conditions is one means of validating the computer codes which are used as input for Army communications systems codes and nuclear weapons effects codes.

SUMMARY

Experimental data from rocket measurements taken in the quiet, daytime D region and simulations of these data by the DAIRCHEM computer code are compared. The purpose is to validate the computer code and to identify those physical processes that need further study.

The direct comparison of simulated and experimental data is shown graphically. It is important to note that no data have been normalized. The total positive ion density profiles show good agreement over the 30 to 90 km region with the exception of the 60 to 75 km span. Possible variations in the absorption of Lyman alpha radiation could account for part of the discrepancy, although it is felt that uncertainties in the formation of negative ions and the total negative ion and electron densities are the cause. Qualitative agreement between predictions of the detailed positive ion composition and in situ mass spectrometric measurements indicate that the positive ion chemistry is being correctly modeled. The computed dominant positive and negative ions are listed as a function of altitude in a table which serves as a guide when comparing these results with other measurements or theoretical calculations.

Comparison of the simulated and experimental electron density profiles shows that the experimentally derived values consistently lie below the predicted ones in the 60 to 85 km region. Mass spectrometer measurements of negative ions (currently available only above 70 km) show little agreement with current predictions in the 70 to 90 km range. These discrepancies indicate that there are electron attachment mechanisms and one or more negative species, possibly small particulates, which are not being correctly modeled.

CONTENTS

INTRODUCTION

The Air Chemistry (AIRCHEM) computer code[1] has been developed to simultaneously solve a large number of stiff, time-dependent, differential equations[2] and thus correctly describe the ion chemistry associated with the nuclearly disturbed atmosphere.[3] A variation of this code, D Region Air Chemistry (DAIRCHEM), has also been developed to model the chemistry of the ionospheric region under both quiet and naturally disturbed conditions.[4] The plan is to compare the predictions of the DAIRCHEM code against experimental data. Reasonable agreement between the measured data and simulations of that data by the DAIRCHEM code serves to validate the code, whereas disagreement indicates which atmospheric processes need further study. Validation of the DAIRCHEM code increases the level of confidence in the AIRCHEM code's predictions for the nuclearly disturbed atmosphere and its potential effects on Army systems.

The case studied here is the daytime, quiet, midlatitude D region. A series of coordinated measurements was made from Wallops Island (37.8° N, 75.5° W) for an extended period of time which covered both quiet and disturbed days. The data selected for comparison were taken on 31 January 1972, a quiet day with no anomalous D region radio absorption. Two rocket flights at 12:30 and 13:05 local time (solar zenith angles of 55° and 58°,

---

[1]E. L. Lortie, M. D. Kregel, and F. E. Niles, 1976, "AIRCHEM: A Computational Technique for Modeling the Chemistry of the Atmosphere," BRL Report 1913 (AD A030157)

[2]T. P. Coffee, J. M. Heimerl, and M. D. Kregel, "A Numerical Method to Integrate Large Stiff Systems of Ordinary Differential Equations," submitted to BRL for publication

[3](see for example) J. M. Heimerl and F. E. Niles, 1978, "BENCHMARK-76: Model Computations for Disturbed Atmospheric Conditions III. Results for Selected Excitation Parameters at 60 km," BRL Technical Report ARBRL-TR-02051 (and references therein).

[4]D. W. Hoock and M. G. Heaps, 1978, "DAIRCHEM: A Computer Code to Model Ionization/Deionization Processes and Chemistry in the Middle Atmosphere," Atmospheric Sciences Laboratory Internal Report, White Sands Missile Range, NM

respectively) provided independent experimental measurements of the electron and total positive ion densities.[5,6,7]

COMPARISONS OF EXPERIMENTAL DATA WITH THE DAIRCHEM SIMULATIONS

The important sources of ionization for the D region are X-rays, Lyman alpha radiation (Lyα) and galactic cosmic rays (GCR). The ion-pair production rates (q) used in the computations[8] are shown in figure 1; the sources were not directly monitored during the rocket measurements. Because 31 January was a quiet day, the X-ray flux was not large, and the direct ionization of NO by Lyα was the largest source of electrons throughout the D region. Due to the rapid attenuation of Lyα by O_2, the dominant source of ionization near 65 km and lower becomes the GCR background. The source of ionization does affect the type of positive ion which is produced. During quiet periods, NO^+ is the most abundant ion initially produced throughout the D region. At 65 km and below, the initially produced ions are N_2^+, O_2^+, N^+, and O^+, in that order;[9] but due to rapid charge exchange and ion-atom interchange processes, the effective ion production rate is approximately 0.8 O_2^+ and 0.2 NO^+ ions per ion pair. The effects on the positive ion chemistry will be discussed in the next section.

---

[5]L. C. Hale, 1974, "Positive Ions in the Mesosphere," COSPAR Methods of Measurements and Results of Lower Ionospheric Structure, K. Rower, ed., 219-235, Akademie-Verlag, Berlin. See also J. D. Mitchell, "An Experimental Investigation of Mesospheric Ionization," Ionospheric Research Scientific Report 416, Pennsylvania State University, 27 June 1973; and T. W. Lai, "Electron Collection Theory for a D-Region Subsonic Blunt Electrostatic Probe," Ionospheric Research Scientific Report 424, Pennsylvania State University, 20 May 1974

[6]L. G. Smith and K. L. Miller, 1978, "The Measurement of O_2 Number Density by Absorption of Lyman Alpha," J Geophys Res, 79:1965-1968

[7]E. A. Mechtly, 1974, "Accuracy of Rocket Measurements of Lower Ionospheric Electron Concentrations," Radio Sci, 9:373-378. See also Progress Report 73-1, p. 62ff, Research in Aeronomy October 1, 1972 - March 31, 1973, edited by Belva Edwards, University of Illinois, Urbana, Illinois, 1973

[8]I. Chidsey, 1978, "SOURCE: A FORTRAN-IV Subroutine Package that Models Several Naturally Occurring Energy Inputs to the Mesosphere," BRL Technical Report, ARBRL-TR-02093

[9]F. Gilmore, as quoted in table 6 in B. F. Myers and M. R. Schoonover, "Electron Energy Degradation in the Atmosphere: Consequent Species and Energy Densities, Electron Flux, and Radiation Spectra," DNA 3513T, 3 January 1975

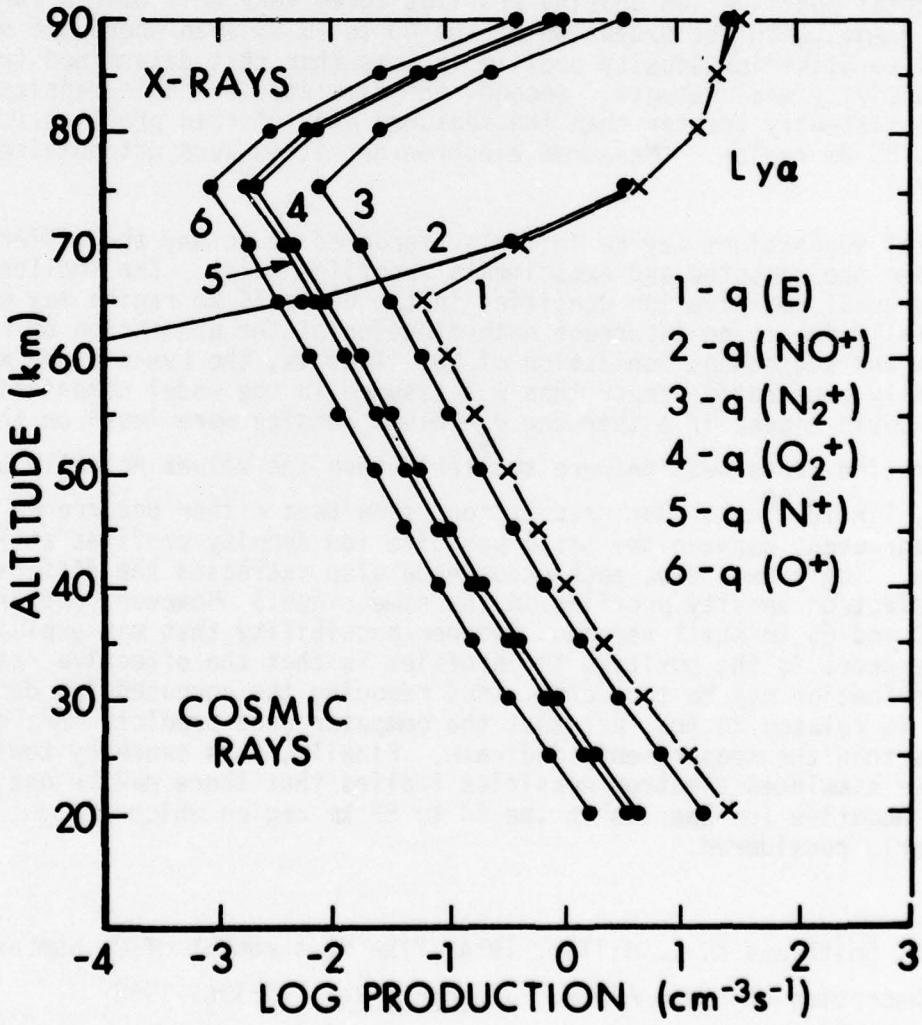

Figure 1. The production rates for electrons and five positive ions as a function of altitude. Direct ionization of NO by Lyman alpha radiation far exceeds the X-ray production above 65 km. Cosmic ray ionization is the source below 65 km.

The electron and total positive ion density profiles computed by using ion pair production rates from figure 1 are shown as circles in figure 2. (Note that the upper scale for the positive ions has been adjusted to the right.) The computed electron densities and total positive ion densities are essentially equal to one another above 65 km. Also shown in figure 2 for comparison are the total positive ion density profile (derived from blunt probe conductivity data), the inferred electron densities from the same data, and the measured electron density profile (combined probe and propagation experiment). We emphasize that the profiles have been simply overlaid; no data have been normalized.

Two general points should be noted when the profiles are compared. First, the total positive ion density profiles agree very well over a large altitude range, with the exception of the 60 to 75 km span where the simulated total positive ion density profile is less than that determined from the conductivity measurements. Second, the simulated electron density profile is consistently greater than the measured and inferred profiles in the 60 to 85 km region. (Measured electron densities were not obtained below 60 km.)

Several suggestions may be initially tendered as to why the differences between the computed and experimental profiles exist. The smaller simulated total positive ion densities in the 60 to 75 km region may be partially due to an incorrect determination of the absorption of Lyman alpha and subsequent ionization of NO. That is, the Lyman alpha may have actually penetrated deeper than was assumed in the model computation. This could happen if either the O_2 column density were less[6] or the O_2 absorption cross section were smaller[10] than the values actually used, i.e., $1 \times 10^{-20} cm^2$. Our calculations show that either occurrence improves the agreement between the total positive ion density profiles at 70 and 75 km. (Unfortunately, each occurrence also increases the differences in the electron density profiles in the same range.) However, differences at 60 and 65 km still remain. Another possibility that may explain the differences in the positive ion profiles is that the effective rate of recombination may be too large, thus reducing the computed ion densities. This is related to the fact that the computer code predicts more electrons than the measurements indicate. Finally, this tendency toward larger simulated electron densities implies that there may be one or more negative ion species in the 60 to 85 km region which are not being properly considered.

---

[6]L. G. Smith and K. L. Miller, 1974, "The Measurement of O_2 Number Density by Absorption of Lyman Alpha," J Geophys Res, 79:1965-1968

[10]J. H. Carver, H. P. Gies, T. I. Hobbs, B. R. Lewis, and D. G. McCoy, 1977, "Temperature Dependence of the Molecular Oxygen Photoabsorption Cross Section Near the H Lyman Alpha Line," J Geophys Res, 82:1955-1960

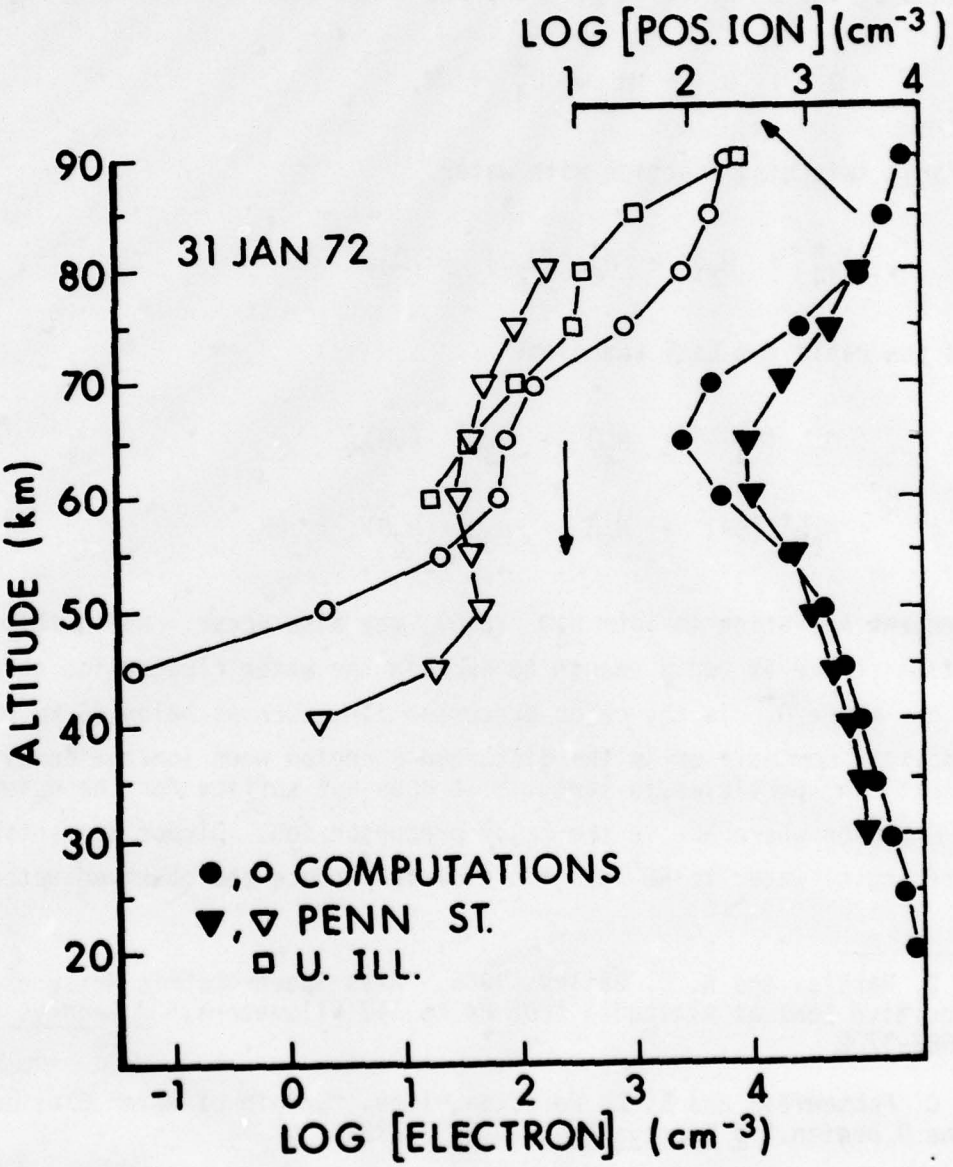

Figure 2. Open symbols are the electron density profiles (bottom scale). Measurements were made by the Pennsylvania State University Group (ref 5) and the University of Illinois Group (ref 7). Solid symbols are the total positive ion profiles (top scale). Measurements were made by the Pennsylvania State University Group (ref 5).

POSITIVE ION CHEMISTRY

The measurement[11] more than a decade ago of water cluster ions in the D region substantially revised our understanding of that portion of the ionosphere. Subsequent laboratory studies[12,13] showed that pathways do exist for converting O_2^+ and NO^+ ions to water cluster ions. The essential points of the O_2^+ reaction path are the three-body clustering of O_2^+ with O_2

$$O_2^+ + O_2 + M \rightarrow O_4^+ + M,$$

a rapid switching reaction with water

$$O_4^+ + H_2O \rightarrow O_2^+ (H_2O) + O_2,$$

and the rapid two-body reactions

$$O_2^+ (H_2O) + H_2O \rightarrow H_3O^+ (OH),$$

$$H_3O^+ (OH) + H_2O \rightarrow H_3O^+ (H_2O) + OH.$$

Subsequent hydration to form $H_3O^+ (H_2O)_n$ may also occur. While this reaction scheme is rapid enough to explain the water cluster ion concentrations where O_2^+ is the major precursor ion, such as below 65 km where cosmic rays dominate or in the disturbed D region when ionization by precipitating particles is large,[14] it does not suffice for the quiet time D region where NO^+ is the major precursor ion. Direct sequential clustering of water to NO^+ was too slow to produce the observed water

---

[11]R. S. Narcisi and A. D. Bailey, 1965, "Mass Spectrometric Measurement of Positive Ions at Altitudes from 64 to 112 Kilometers," J Geophys Res, 70:3687-3700

[12]F. C. Fehsenfeld and E. E. Ferguson, 1969, "Origin of Water Cluster Ions in the D Region," J Geophys Res, 74:2217-2222

[13]F. C. Fehsenfeld, M. Mosesman, and E. E. Ferguson, 1971, "Ion Molecule Reactions in an $O_2^+ - H_2O$ System," J Chem Phys, 55:2115-2119

[14]G. C. Reid, 1972, "The D Region During PCA Conditions," Magnetosphere Ionospheric Interactions, K. Folkstad, ed., 39-46, Universitets-forlaget, Oslo

cluster densities. More rapid switching reactions have been proposed[15,16] of the type

$$NO^+ + N_2 + M \rightarrow NO^+ (N_2) + M,$$

$$NO^+ (N_2) + CO_2 \rightarrow NO^+ (CO_2) + N_2,$$

$$NO^+ (CO_2) + H_2O \rightarrow NO^+ (H_2O) + CO_2,$$

with a similar sequence until the third hydrate is produced. The third hydrate then undergoes a rapid two-body reaction with water

$$NO^+ (H_2O)_3 + H_2O \rightarrow H_3O^+ (H_2O)_2 + HNO_2,$$

and the hydronium ion sequence is entered.[17,18]

Repeated rocket measurements over a wide variety of latitudes and seasons have shown that the hydronium ion clusters $H_3O^+ (H_2O)_n$ begin to rapidly

---

[15]F. E. Niles and J. M. Heimerl, 1972, "Association, Switching and Rearrangement for Positively Charged Cluster Ions in the Upper Atmosphere, I: Qualitative Description," BRL Report 1595

[16]J. M. Heimerl, J. A. Vanderhoff, L. J. Pucket, G. E. Keller, and F. E. Niles, 1972, "Association, Switching and Rearrangement for Positively Charged Cluster Ions, II: Applications at 80 km," BRL Report 1605

[17]G. C. Reid, 1976, "Ion Chemistry in the D Region," Advances in Atomic and Molecular Physics, 12:375-414, Academic Press, New York

[18]G. C. Reid, 1977, "The Production of Water-Cluster Positive Ions in the Quiet Daytime D Region," Planet Space Sci, 25:275-290

decrease in density above about 75 to 85 km.[11,19-21] The main reason is that the clustering sequence involves several three-body reactions with major constituents and therefore rapidly decreases in efficiency with increasing altitude. The exact shape of the H_3O^+ water cluster ion profile is also somewhat a function of the temperature and water vapor profiles. Above 75 to 85 km, one might expect to see a few of the "early" clusters in the NO^+ and O_2^+ ion hydration chains.

The simulated positive ion density profiles are shown in figures 3 and 4 for ions having, respectively, NO^+ and H_3O^+ as the core ions. Also shown is the predicted total positive ion density profile. As expected, the computer code predicts that NO^+ and its first two water clusters, along with the intermediate cluster $NO^+ (CO_2)$, dominate the upper D Region. There is good qualitative agreement between these predictions and several mass spectrometric measurements;[19-22] nevertheless, these clusters are weakly bound and therefore subject to collisional breakup from the in situ rocket measurement techniques. Figure 4 shows the computed density profiles for the H_3O^+ hydrates. Above 65 km, entry to the hydronium ion chain is through NO^+ producing $H_3O^+ (H_2O)_2$, while below 65 km, entry is through O_2^+ producing $H_3O^+ (H_2O)$. The code predicts that clustering to heavier hydrates will be important below 75 km. Again, the comparison with mass spectrometric measurements gives good qualitative agreement.

---

[11]R. S. Narcisi and A. D. Bailey, 1965, "Mass Spectrometric Measurements of Positive Ions at Altitudes from 64 to 112 Kilometers," J Geophys Res, 70:3687-3700

[19]D. Krankowsky, F. Arnold, H. Weider, J. Kissel, and J. Zähringer, 1972, "Positive Ion Composition in the Lower Ionosphere," Radio Sci, 7:93-98

[20]R. S. Narcisi, A. D. Bailey, L. E. Wlodyka, and C. R. Philbrick, 1972, "Ion Composition Measurements in the Lower Ionosphere During the November 1966 and March 1970 Solar Eclipses," J Atmos Terr Phys, 34:647-658

[21]A. Johannessen and D. Krankowsky, 1974, "Daytime Positive Ion Composition Measurement in the Altitude Range 73 - 137 km above Sardinia," J Atmos Terr Phys, 36:1233-1247

[22]F. Arnold and D. Krankowsky, "A New Concept for the D Region Ion Chemistry as Inferred from a Mass Spectrometer Measurement," paper presented at International Symposium on Solar-Terrestrial Physics, COSPAR, Sao Paulo, Brazil, 1974

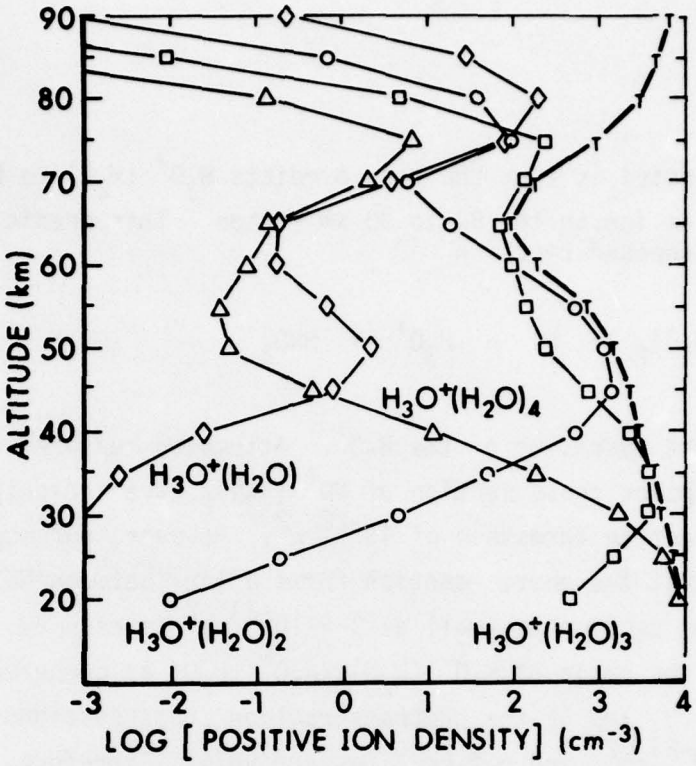

Figure 3. Computed positive ion density profiles for species that have NO^+ as their core ion. The total positive ion profile is given by the heavy curve marked "T."

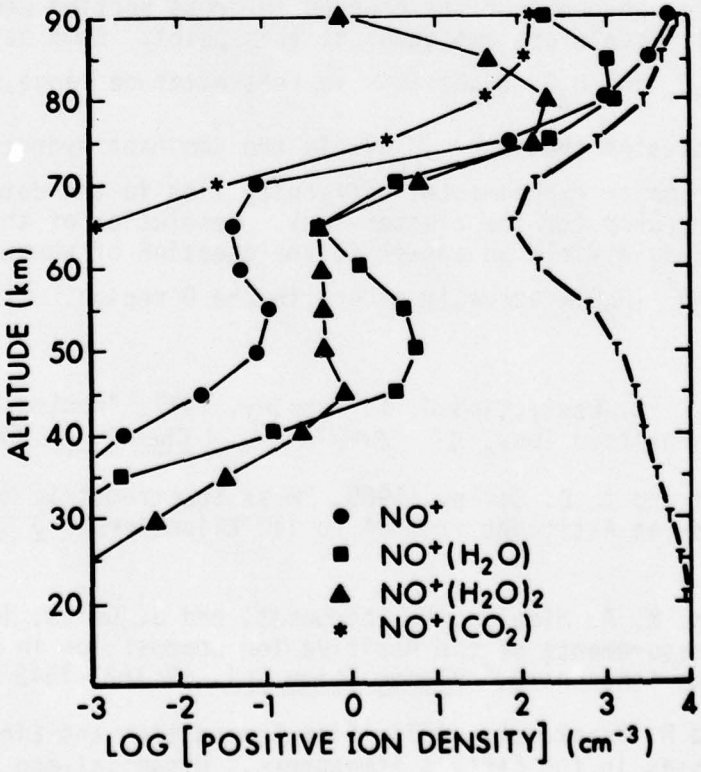

Figure 4. Computed positive ion density profiles for species that have H_3O^+ as their core ion. The total positive ion profile is given by the heavy curve marked "T."

One point to be noted is that the code predicts $H_3O^+ (H_2O)$ to be the dominant hydronium ion in the 80 to 90 km region. This prediction is because of the proposed reaction

$$NO^+ (H_2O)_2 + h\nu \rightarrow H_3O^+ + HNO_2$$

and the subsequent hydration of the H_3O^+. Attempted measurements[23] of the photon absorption cross section of $NO^+ (H_2O)_2$ have indicated that it is below the detection threshold of $10^{-20} cm^2$. However, our modeling calculations show that the above reaction forms a link between NO^+ and H_3O^+ even when a cross section as small as $2 \times 10^{-21} cm^2$ is assumed. Specifically, at 80 km the ratio of $H_3O^+ (H_2O)_2 / H_3O^+ (H_2O)$ as computed from the model is 0.06, 1.3, and 12 for photodestruction cross sections of $2 \times 10^{-19} cm^2$, $2 \times 10^{-21} cm^2$, and 0.0 cm^2, respectively. Therefore, relative ratio of the hydrates of H_3O^+ is a sensitive indicator of the importance of the photolysis of $NO^+ (H_2O)_2$ (whereas the total positive ion density varies only a few percent for the changes in cross section used above). Rocket ion measurements are ambiguous at this point. Some have shown an abundance of H_3O^+ and $H_3O^+ (H_2O)$ ions in this altitude range,[11,24] while others have indicated that $H_3O^+ (H_2O)_2$ is the dominant hydronium ion cluster.[25] The major experimental difficulty lies in the determination of the degree of breakup for the cluster ions. Resolution of this experimental problem could yield an answer to the question of whether the photolysis of $NO^+ (H_2O)_2$ actually occurs in the D region.

---

[23]G. P. Smith, P. C. Cosby, and J. T. Moseley, 1977, "Photodissociation of Atmospheric Positive Ions, I: 5300-6700Å, J Chem Phys, 67:3818-3828

[11]R. S. Narcisi and A. D. Bailey, 1965, "Mass Spectrometric Measurements of Positive Ions at Altitudes from 64 to 112 Kilometers," J Geophys Res, 70:3687-3700

[24]P. A. Zbinden, M. A. Hidalgo, P. Eberhardt, and J. Geiss, 1975, "Mass Spectrometer Measurements of the Positive Ion Composition in the D and E Regions of the Ionosphere," Planet Space Sci, 23:1621-1642

[25]F. Arnold and D. Krankowsky, 1977, "Ion Composition and Electron and Ion Loss Processes in the Earth's Atmosphere," Dynamical and Chemical Coupling, 93-127, B. Grandal and J. Holtet, eds., Dr. Reidel, Dordrecht

Figure 5 illustrates the summed profiles for the two main ion groupings -- the one with NO^+ as the core ion and the other with the H_3O^+ as the core ion. The crossover point between the two groupings is 75 km, which is in reasonable agreement with experimental observations. Figure 5 shows that the region of 60 to 75 km, where the simulated total positive ion profile is less than the experimentally determined one (see figure 2), is clearly dominated by H_3O^+ cluster ions. As mentioned in the previous section, one possible reason for the lower simulated ion densities is that the effective recombination rate may be too large. This large recombination rate may in turn have two causes. One cause may be that the code predicts multiple-cluster ions which are larger (in mass) than the ones which were actually present. If the dominant cluster ion were $H_3O^+ (H_2O)$ rather than the predicted $H_3O^+ (H_2O)_3$, the electron ion recombination coefficient would be half as large. Nominally this would increase both the ion and electron densities approximately 40 percent, which would improve the comparison between the ion profiles but increase the discrepancy between the electron profiles. Other experimental determinations of exact ion composition are still subject to interpretation. Some measurements[20,24] indicate that $H_3O^+ (H_2O)$ may be the predominant positive ion in the lower D region, while other experiments[11,25] show that the heavier clusters dominate. Until the question of cluster breakup is resolved, we adopt the position that the code correctly predicts the heavier positive ion clusters. The other cause of a too-large effective recombination rate may be in the negative ion concentrations and negative ion to electron ratio. As a "rule-of-thumb," the ion-ion recombination coefficients are one to two orders of magnitude smaller than electron-ion recombination

---

[20]R. S. Narcisi, A. D. Bailey, L. E. Wlodyka, and C. R. Philbrick, 1972, "Ion Composition Measurements in the Lower Ionosphere During the November 1966 and March 1970 Solar Eclipses," J Atmos Terr Phys, 34:647-658

[24]P. A. Zbinden, M. A. Hidalgo, P. Eberhardt, and J. Geiss, 1975, "Mass Spectrometer Measurements of the Positive Ion Composition in the D and E Regions of the Ionosphere," Planet Space Sci, 23:1621-1642

[11]R. S. Narcisi and A. D. Bailey, 1965, "Mass Spectrometric Measurement of Positive Ions at Altitudes from 64 to 112 Kilometers," J Geophys Res, 70:3687-3700

[25]F. Arnold and D. Krankowsky, 1977, "Ion Composition and Electron and Ion Loss Processes in the Earth's Atmosphere," Dynamical and Chemical Coupling, 93-127, B. Grandal and J. Holtet, eds., Dr. Reidel, Dordrecht

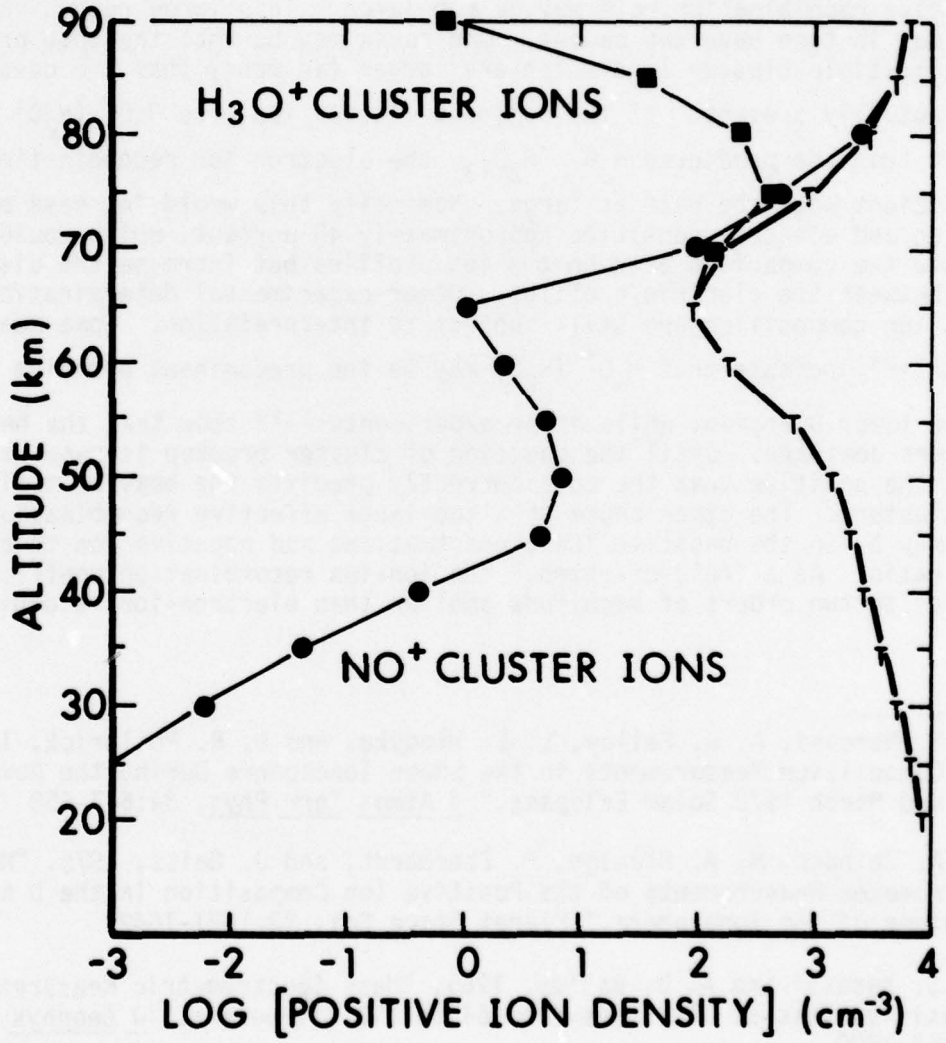

Figure 5. NO^+ cluster ions and H_3O cluster ions represent the sums of the profiles of figures 3 and 4, respectively. Below 65 km the total positive ions are very well approximated by the H_3O^+ core cluster ions, above 85 km by the NO^+ core cluster ions.

coefficients.[26,27] Thus, an appreciable concentration of negative ions in the 60 and 75 km region would increase the simulated positive ion densities and thus improve the agreement of the two positive ion profiles in figure 2, while also possibly reconciling some of the differences between the simulated and experimentally determined electron profiles. This idea will be explored further in the next section.

NEGATIVE ION CHEMISTRY

The major formation process for the initial negative ion is the three-body attachment of electrons to O_2

$$e + O_2 + M \rightarrow O_2^- + M.$$

However, there are also rapid detachment processes for O_2^-

$$O_2^- + O \rightarrow O_3 + e,$$

$$O_2^- + O_2\left(^1\Delta_g\right) \rightarrow 2O_2 + e,$$

which tend to limit the O_2^- density in the upper D region. The next important step in the formation of more complex and stable negative ions is a charge exchange reaction between O_3 and O_2^-

$$O_2^- + O_3 \rightarrow O_3^- + O_2,$$

---

[26]D. Smith, N. G. Adams, and M. J. Church, 1976, "Mutual Neutralization Rates of Ionospherically Important Ions," Planet Space Sci, 24:697-703

[27]D. Smith and M. J. Church, 1977, "Ion-Ion Recombination Rates in the Earth's Atmosphere," Planet Space Sci, 25:433-439

followed by the reaction

$$O_3^- + CO_2 \rightarrow CO_3^- + O_2.$$

The CO_3^- ion, however, is also dissociated by atomic oxygen

$$CO_3^- + O \rightarrow O_2^- + CO_2$$

which short circuits the negative ion formation process back to the O_2^- ion. The next major step is the reaction

$$CO_3^- + NO \rightarrow NO_2^- + CO_2$$

which is followed by the reaction

$$NO_2^- + O_3 \rightarrow NO_3^- + O_2$$

to form the negative ion with the largest electron affinity, NO_3^-.

The major paths along which the charge flows are illustrated in figure 6. Although there are numerous other reactions which enter in, the main sequence has been outlined above. Of interest is the secondary path of O_2^- clustering to form O_4^- which in turn switches with CO_2 to form CO_4^-. While this is not a major path for the flow of charge, appreciable buildup of the CO_4^- ion can occur because of its small photodissociation cross section.[28,29] Hydration reactions occur for essentially all of the

---

[28]G. P. Smith, L. C. Lee, P. C. Cosby, J. R. Peterson, and J. T. Moseley, 1978, "Photodissociation and Photodetachment of Molecular Negative Ions, V: Atmospheric Ions from 7000 to 8400 Å," J Chem Phys, 68:3818-3822

[29]M. L. Vestal and G. H. Mauclaire, 1977, "Photodissociation of Negative Ions Formed in CO_2 and CO_2/O_2 Mixtures," J Chem Phys, 67:3758-3766

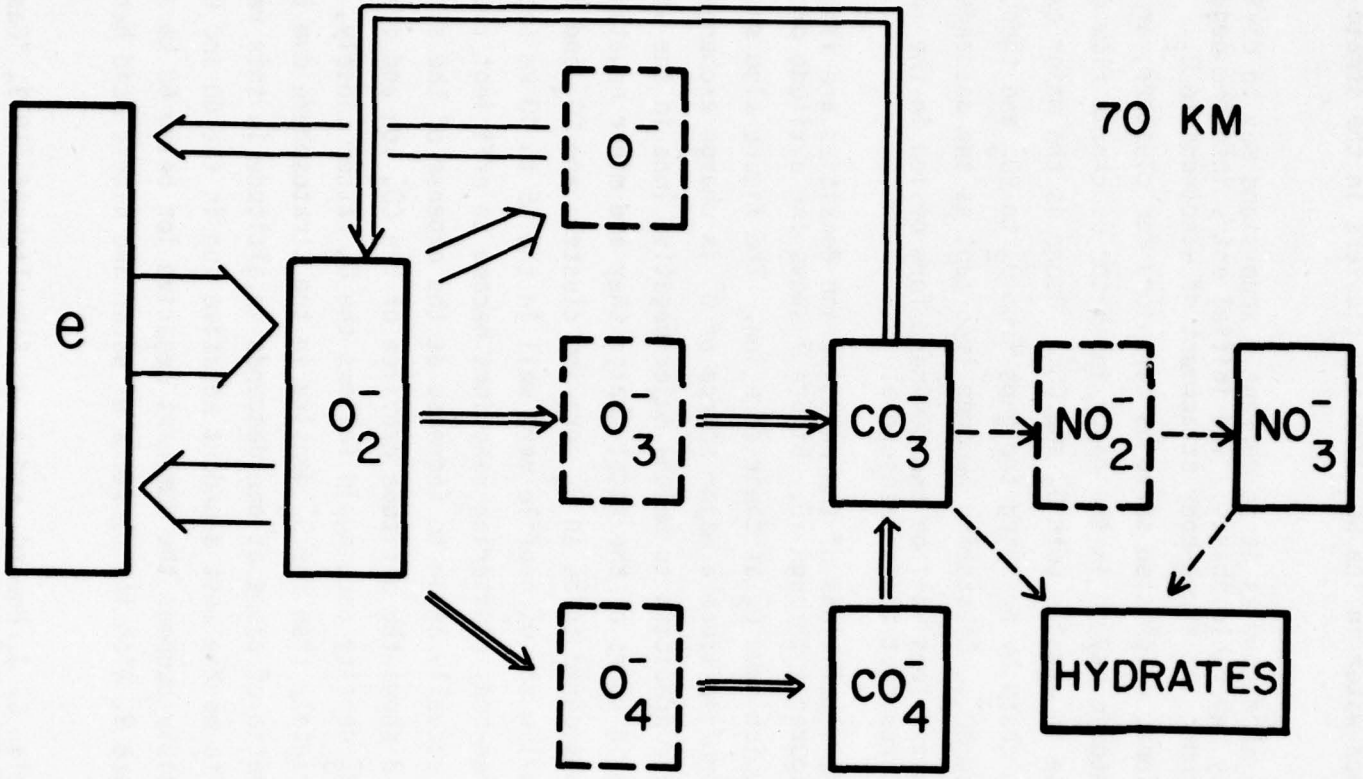

NEGATIVE ION FLOW CHART

Figure 6. Major paths for flow of negative charge down the negative ion chain. Solid boxes indicate ions with appreciable concentrations; dashed-line boxes indicate important intermediary ions which have very small concentrations.

negative species, with hydrated forms of the ions expected to be dominant at lower altitudes. Chemical considerations indicated that nitric acid, HNO_3, will replace water in the NO_3^- core ion clusters in the stratosphere.[30,31]

The negative ion chemistry as it is currently understood may be divided into conveniently separable phases. The initial entry into the negative ion chain is through the three-body attachment of electrons to O_2. The major negative ions, which also serve as core ions for clusters, are O_2^-, CO_3^-, and NO_3^-. Atomic oxygen is the major inhibitor of charge flow down the chain because it attacks both O_2^- and CO_3^-. Ozone is the major expeditor of flow down the chain by bridging the gaps from O_2^- to CO_3^- and then, with the aid of NO, to NO_3^-. Clustering becomes important as one descends in altitude and cluster ions will be the dominant form of ion in the lower mesosphere and throughout the stratosphere.

The computer code simulations of the negative ion densities are illustrated in the set of figures 7 through 10. Figure 7 shows the altitude profiles for those ions which have O_2^- as their core ion. The figure also shows the O^- ion density profile since a major source of O^- is charge exchange with O_2^-. O^- and O_2^- are predicted to be the major negative ions in the upper D region, although in terms of the total charge they are minor negative species. CO_4^- is considered to be an O_2^- core ion cluster; and CO_4^- and its water cluster follow the O_2^- profile very well in the 65 to 40 km region. Below 40 km, three-body clustering reactions become so efficient that CO_4^- and its hydrate actually begin to increase at the expense of the simpler O_2^- ion. Figure 8 shows the altitude profiles of the CO_3^- ion and its water cluster. The CO_3^- density once again follows the O_2^- rather closely, but decreases less rapidly than the O_2^- density in the stratosphere due to the increasing ratio of ozone as one descends in altitude in this region. CO_3^- is computed to be the most abundant negative ion in the 60 and 65 km region. NO_3^- rapidly becomes the dominant negative ion below 60 km as is shown in figure 9, with its clusters of water and nitric acid becoming

---

[30]F. C. Fehsenfeld, C. J. Howard, and A. J. Schmeltekopf, 1973, "Gas Phase Ion Chemistry of HNO_3," J Chem Phys, 63:2835-2841

[31]J. C. Harris, D. G. Moos, N. R. W. Swann, G. F. Neill, and P. Gildwarg, 1976, "Simultaneous Measurements of H_2O, NO_2, and HNO_3 in the Daytime Stratosphere from 15 to 35 km," Nature, 259:300-301

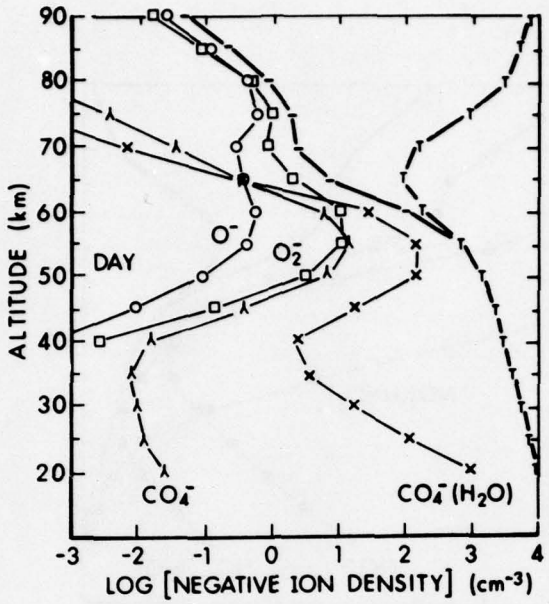

Figure 7. Profiles of negative ions that have O_2^- as their core; CO_4^- is taken to be O_2^- (CO_2). O profile is also shown. The total positive ion profile is given by the heavy line marked "T." Above 55 km the total negative ion profile is shown by "-." Below 55 km the total positive and total negative profiles overlap.

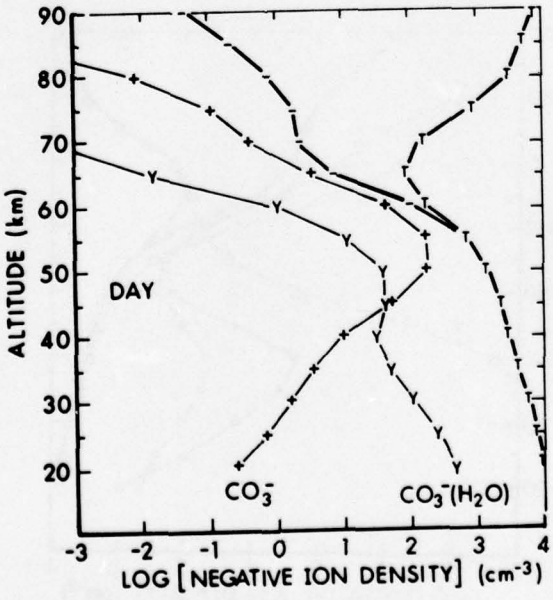

Figure 8. Profiles of the negative ions that have CO_3^- as their core ion. The total negative ion profile is shown by the heavy line marked "-" above 55 km and "T" below 55 km.

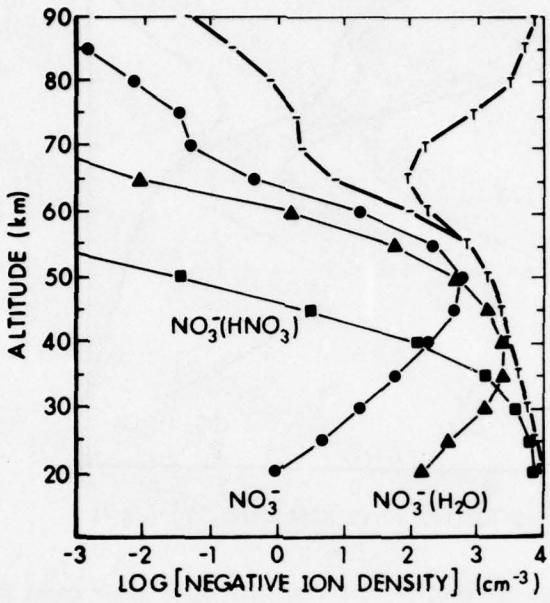

Figure 9. Profiles of the negative ions that have NO_3^- as their core ion. The total negative ion profile is shown by the heavy line marked "-" above 55 km and "T" below 55 km.

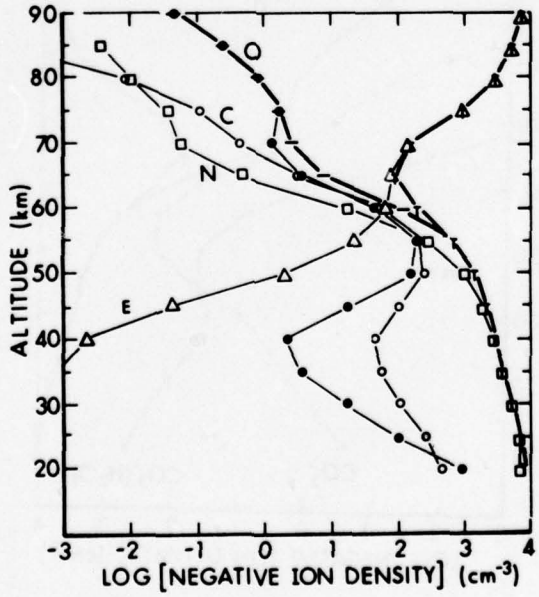

Figure 10. O, C, and N represent the profiles of the sums of the negative ions that are given in figures 7, 8, and 9, respectively. The electron density profile, E, is also shown.

the more important ions in the stratosphere. Only one molecule each of water and nitric acid were clustered to NO_3^- in this model. More complex and mixed clusters have not been included at the present but most probably do exist in nature.

Figure 10 shows the three groups of negative ions, O_2^-, CO_3^- and NO_3^-, and the total charge. These groupings do not show the sharp distinctions with altitude that the NO^+ and H_3O^+ groups did in figure 5, but the transitions from O_2^- to CO_3^- to NO_3^- groupings are still apparent as one descends in altitude. Table 1 lists the dominant positive and negative species and their corresponding altitude ranges. Certain features should be noted when figures 5 and 10 are compared. First, clustering to positive ions is an important process throughout the entire D region, whereas clustering to negative ions only becomes dominant below 60 km. Secondly, the total negative ion density quickly decreases above 60 km. These features are due mainly to the fact that the negative ions O_2^- and CO_3^- are attacked by atomic oxygen, whose density increases with altitude, and to the fact that the formation of the more stable negative ions depends on ozone, whose density decreases with altitude. The DAIRCHEM computer code therefore predicts small negative ion densities in the D region.

Comparison of the code's predictions with available experimental data is somewhat disquieting. Mass spectrometer measurements have indicated the presence of negative ions throughout the D region,[32,33,20] although the absolute concentrations are still in question. Rapid decreases in the negative ion density with increasing altitude have been observed in the vicinity of 78 and 90 km, whereas the code predicts that the negative ion density begins to decrease above the much lower altitude of 60 km. The presence of heavy negative ion clusters, often with masses greater than 150 u, has been experimentally inferred in the 70 to 90 km region.[20,32] The code predicts only the simple negative ions, O_2^-, O^-, CO_3^-, and NO_3^-,

---

[32]R. S. Narcisi, A. D. Bailey, L. Della Lucca, C. Sherman, and D. M. Thomas, 1971, "Mass Spectrometric Measurements of Negative Ions in the D and Lower E Regions," J Atmos Terr Phys, 33:1147-1159

[33]F. Arnold, J. Kissle, D. Krankowsky, H. Wieder, and J. Zähringer, 1971, "Negative Ions in the Lower Ionosphere: A Mass Spectrometric Measurement," J Atmos Terr Phys, 33:1169-1175

[20]R. S. Narcisi, A. D. Bailey, L. E. Wlodyka, and C. R. Philbrick, 1972, "Ion Composition Measurements in the Lower Ionosphere During the November 1966 and March 1970 Solar Eclipses," J Atmos Terr Phys, 34:647-658

TABLE 1. QUIET TIME D REGION

Altitude Range (km)	Dominant Negative Ion	Dominant Positive Ion
85-90	O^-	NO^+
80-85	O_2^- , O^-	$NO^+(H_2O)$, NO^+
75-80	O_2^-	$H_3O^+(H_2O)_n$, $NO^+(H_2O)$
70-75	O_2^-	$H_3O^+(H_2O)_n$
65-70	CO_3^- , O_2^-	"
60-65	CO_3^-	"
55-60	NO_3^- , CO_3^-	"
50-55	NO_3^-	"
40-50	$NO_3^-(H_2O)$, NO_3^-	"
30-40	$NO_3^-(HNO_3)$, $NO_3^-(H_2O)$	"
20-30	$NO_3^-(HNO_3)$	"

in this region. The electron and total positive ion density profiles shown in figure 2, which were derived from independent rocket measurements, imply an increasing negative ion density in the 60 and 85 km region which equals and even exceeds the electron density. Again the known ion chemistry predicts a decreasing negative ion density in this region.

It has become evident at this point that, in contrast to the positive ion chemistry, there are several major uncertainties in connection with the negative ion chemistry and the resultant electron and negative ion densities. Several suggestions can be made which may help to reconcile or at least better define the current uncertainties.

When the rocket measurements yielding the data shown in figure 2 were made, there were no simultaneous measurements of ozone and atomic oxygen made. Considering the importance of these minor neutral species in the formation of negative ions, detailed profiles in the 60 to 90 km region would be helpful. The DAIRCHEM code does determine representative $[O_3]$ and $[O]$ profiles based on time-dependent photochemical considerations, so that the major effects are already accounted for. Detailed comparisons with experimental profiles would help to resolve questions concerning the exact altitudes of negative ion formation, but would not resolve major discrepancies involving total negative ion concentrations.

The comparison of computer code results and experimental data would strongly imply that there is another method of negative ion formation other than the known three-body attachment of electrons to O_2. The difference between the measured electron and total positive ion densities in figure 2 also suggests that a negative species not currently modeled is present in the D region. The presence of ice particulates of submicron size has been suggested[34] as a means of providing an alternate electron attachment mechanism and negative species. Analysis[35] and modeling[36] of data from the 1966 solar eclipse have yielded similar conclusions.[37] The previously mentioned

---

[34]E. T. Chesworth and L. C. Hale, "Ice Particulates in the Mesosphere," 1974, Geophys Res Letters, 1:347-350

[35]R. D. Sears, 1972, "Analysis of the 1966 Solar Eclipse Data," LMSC D246526 (DNA 2863F), Lockheed, Palo Alto Research Laboratory

[36]M. G. Heaps, F. E. Niles, and R. D. Sears, 1978, "Modeling the Ion Chemistry of the D Region: A Case Study Based Upon the 1966 Total Solar Eclipse," ASL-TR-0015, Atmospheric Sciences Laboratory, White Sands Missile Range, NM

[37]M. G. Heaps, "Inclusion of Small Particulates to Explain Variations of D Region Electron Densities Observed During a Solar Eclipse," ASL-TR (in preparation)

measurements of heavy negative ions also lend indirect support to the possible role of small particulates in D region processes. An area of further study would be electron attachment/detachment processes, ion clustering and growth mechanisms, and the influence of nongas-phase chemistry in the lower ionosphere.

CONCLUSION

The positive ion chemistry portion of the DAIRCHEM computer code may be considered to be validated by this comparison. In need of further study are electron attachment/detachment processes and the possible role of particulates in D region ion chemistry.

REFERENCES

1. Lortie, E. L., M. D. Kregel, and F. E. Niles, 1976, "AIRCHEM: A Computational Technique for Modeling the Chemistry of the Atmosphere," BRL Report 1913 (AD A030157).

2. Coffee, T. P., J. M. Heimerl, and M. D. Kregel, "A Numerical Method to Integrate Large Stiff Systems of Ordinary Differential Equations," submitted to BRL for publication.

3. (see for example) J. M. Heimerl and F. E. Niles, 1978, "BENCHMARK-76: Model Computations for Disturbed Atmospheric Conditions III. Results for Selected Excitation Parameters at 60 km," BRL Technical Report ARBRL-TR-02051 (and references therein).

4. Hoock, D. W., and M. G. Heaps, 1978, "DAIRCHEM: A Computer Code to Model Ionization/Deionization Processes and Chemistry in the Middle Atmosphere," Atmospheric Sciences Laboratory Internal Report, White Sands Missile Range, NM.

5. Hale, L. C., 1974, "Positive Ions in the Mesosphere," COSPAR Methods of Measurements and Results of Lower Ionospheric Structure, K. Rower, ed., 219-235, Akademie-Verlag, Berlin. See also J. D. Mitchell, "An Experimental Investigation of Mesospheric Ionization," Ionospheric Research Scientific Report 416, Pennsylvania State University, 27 June 1973; and T. W. Lai, "Electron Collection Theory for a D Region Subsonic Blunt Electrostatic Probe," Ionospheric Research Scientific Report 424, Pennsylvania State University, 20 May 1974.

6. Smith, L. G., and K. L. Miller, 1974, "The Measurement of O_2 Number Density by Absorption of Lyman Alpha," J Geophys Res, 79:1965-1968.

7. Mechtly, E. A., 1974, "Accuracy of Rocket Measurements of Lower Ionospheric Electron Concentrations," Radio Sci, 9:373-378. See also Progress Report 73-1, p 62ff, Research in Aeronomy 1 October 1972 - 31 March 1973, edited by Belva Edwards, University of Illinois, Urbana, Illinois, 1973.

8. Chidsey, I., 1978, "SOURCE: A FORTRAN-IV Subroutine Package that Models Several Naturally Occurring Energy Inputs to the Mesosphere," BRL Technical Report, ARBRL-TR-02093.

9. Gilmore, F., as quoted in table 6 in B. F. Myers and M. R. Schoonover, "Electron Energy Degradation in the Atmosphere: Consequent Species and Energy Densities, Electron Flux, and Radiation Spectra," DNA 35135, 3 January 1975.

10. Carver, J. H., H. P. Gies, T. I. Hobbs, B. R. Lewis, and D. G. McCoy, 1977, "Temperature Dependence of the Molecular Oxygen Photoabsorption Cross Section Near the H Lyman Alpha Line," J Geophys Res, 82:1955-1960.

11. Narcisi, R. S., and A. D. Bailey, 1965, "Mass Spectrometric Measurements of Positive Ions at Altitudes from 64 to 112 Kilometers," J Geophys Res, 70:3687-3700.

12. Fehsenfeld, F. C., and E. E. Ferguson, 1969, "Origin of Water Cluster Ions in the D Region," J Geophys Res, 74:2217-2222.

13. Fehsenfeld, F. C., M. Mosesman, and E. E. Ferguson, 1971, "Ion Molecule Reactions in an $O_2^+ - H_2O$ System," J Chem Phys, 55:2115-2119.

14. Reid, G. C., 1972, "The D Region During PCA Conditions," Magnetosphere Ionospheric Interactions, K. Folkstad, ed., 39-46, Universitetsforlaget, Oslo.

15. Niles, F. E., and J. M. Heimerl, 1972, "Association, Switching and Rearrangement for Positively Charged Cluster Ions in the Upper Atmosphere, I: Qualitative Description," BRL Report 1595.

16. Heimerl, J. M., J. A. Vanderhoff, L. J. Pucket, G. E. Keller, and F. E. Niles, 1972, "Association, Switching and Rearrangement for Positively Charged Cluster Ions, II: Applications at 80 km," BRL Report 1605.

17. Reid, G. C., 1976, "Ion Chemistry in the D Region," Advances in Atomic and Molecular Physics, 12:375-414, Academic Press, New York.

18. Reid, G. C., 1977, "The Production of Water cluster Positive Ions in the Quiet Daytime D Region," Planet Space Sci, 25:275-290.

19. Krankowsky, D., F. Arnold, H. Weider, J. Kissel, and J. Zähringer, 1972, "Positive Ion Composition in the Lower Ionosphere," Radio Sci, 7:93-98.

20. Narcisi, R. S., A. D. Bailey, L. E. Wlodyka, and C. R. Philbrick, 1972, "Ion Composition Measurements in the Lower Ionosphere During the November 1966 and March 1970 Solar Eclipses," J Atmos Terr Phys, 34:647-658.

21. Johannessen, A., and D. Krankowsky, 1974, "Daytime Positive Ion Composition Measurement in the Altitude Range 73-127 km above Sardinia," J Atmos Terr Phys, 36:1233-1247.

22. Arnold, F., and D. Krankowsky, "A New Concept for the D Region Ion Chemistry as Inferred from a Mass Spectrometer Measurement," paper presented at International Symposium on Solar-Terrestrial Physics, COSPAR, Sao Paulo, Brazil, 1974.

23. Smith, G. P., P. C. Cosby, and J. T. Moseley, 1977, "Photodissociation of Atmospheric Positive Ions, I: 5300-6700Å, J Chem Phys, 67:3818-3828.

24. Zbinden, P. A., M. A. Hildalgo, P. Eberhardt, and J. Geiss, 1975, "Mass Spectrometer Measurements of the Positive Ion Composition in the D and E Regions of the Ionosphere," Planet Space Sci, 23:1621-1642.

25. Arnold, F., and D. Krankowsky, 1977, "Ion Composition and Electron and Ion Loss Processes in the Earth's Atmosphere," Dynamical and Chemical Coupling, 93-127, B. Grandal and J. Holtet, eds., Dr. Reidel, Dordrecht.

26. Smith, D., N. G. Adams, and M. J. Church, 1976, "Mutual Neutralization Rates of Ionospherically Important Ions," Planet Space Sci, 24:697-703.

27. Smith, D., and M. J. Church, 1977, "Ion-Ion Recombination Rates in the Earth's Atmosphere," Planet Space Sci, 25:433-439.

28. Smith, G. P., L. C. Lee, P. C. Cosby, J. R. Peterson, and J. T. Moseley, 1978, "Photodissociation and Photodetachment of Molecular Negative Ions, V: Atmospheric Ions from 7000 to 8400 Å," J Chem Phys, 68:3818-3822.

29. Vestal, M. L., and G. H. Mauclaire, 1977, "Photodissociation of Negative Ions Formed in CO_2 and CO_2/O_2 Mixtures," J Chem Phys, 67:3758-3766.

30. Fehsenfeld, F. C., C. J. Howard, and A. J. Schmeltekopf, 1973, "Gas Phase Ion Chemistry of HNO_3," J Chem Phys, 63:2835-2841.

31. Harris, J. C., D. G. Moos, N. R. W. Swann, G. F. Neill, and P. Gildwarg, 1976, "Simultaneous Measurements of H_2O, NO_2, and HNO_3 in the Daytime Stratosphere from 15 to 35 km," Nature, 259:300-301.

32. Narcisi, R. S., A. D. Bailey, L. Della Lucca, C. Sherman, and D. M. Thomas, 1971, "Mass Spectrometric Measurements of Negative Ions in the D and Lower E Regions," J Atmos Terr Phys, 33:1147-1159.

33. Arnold, F., J. Kissel, D. Krankowsky, H. Wieder, and J. Zähringer, 1971, "Negative Ions in the Lower Ionosphere: A Mass Spectrometric Measurement," J Atmos Terr Phys, 33:1169-1175.

34. Chesworth, E. T., and L. C. Hale, "Ice Particulates in the Mesosphere," 1974, Geophys Res Letters, 1:347-350.

35. Sears, R. D., 1972, "Analysis of the 1966 Solar Eclipse Data," LMSC D246526 (DNA 2863F), Lockheed, Palo Alto Research Laboratory.

36. Heaps, M. G., F. E. Niles, and R. D. Sears, 1978, "Modeling the Ion Chemistry of the D Region: A Case Study Based Upon the 1966 Total Solar Eclipse," ASL-TR-0015, Atmospheric Sciences Laboratory, White Sands Missile Range, NM.

37. Heaps, M. G., "Inclusion of Small Particulates to Explain Variations of D Region Electron Densities Observed During a Solar Eclipse," ASL-TR (in preparation).

DISTRIBUTION LIST

Dr. Frank D. Eaton
Geophysical Institute
University of Alaska
Fairbanks, AK 99701

Commander
US Army Aviation Center
ATTN: ATZQ-D-MA
Fort Rucker, AL 36362

Chief, Atmospheric Sciences Div
Code ES-81
NASA
Marshall Space Flight Center,
AL 35812

Commander
US Army Missile R&D Command
ATTN: DRDMI-CGA (B. W. Fowler)
Redstone Arsenal, AL 35809

Redstone Scientific Information Center
ATTN: DRDMI-TBD
US Army Missile R&D Command
Redstone Arsenal, AL 35809

Commander
US Army Missile R&D Command
ATTN: DRDMI-TEM (R. Haraway)
Redstone Arsenal, AL 35809

Commander
US Army Missile R&D Command
ATTN: DRDMI-TRA (Dr. Essenwanger)
Redstone Arsenal, AL 35809

Commander
HQ, Fort Huachuca
ATTN: Tech Ref Div
Fort Huachuca, AZ 85613

Commander
US Army Intelligence Center & School
ATTN: ATSI-CD-MD
Fort Huachuca, AZ 85613

Commander
US Army Yuma Proving Ground
ATTN: Technical Library
Bldg 2100
Yuma, AZ 85364

Naval Weapons Center (Code 3173)
ATTN: Dr. A. Shlanta
China Lake, CA 93555

Sylvania Elec Sys Western Div
ATTN: Technical Reports Library
PO Box 205
Mountain View, CA 94040

Geophysics Officer
PMTC Code 3250
Pacific Missile Test Center
Point Mugu, CA 93042

Commander
Naval Ocean Systems Center (Code 4473)
ATTN: Technical Library
San Diego, CA 92152

Meteorologist in Charge
Kwajalein Missile Range
PO Box 67
APO San Francisco, CA 96555

Director
NOAA/ERL/APCL R31
RB3-Room 567
Boulder, CO 80302

Library-R-51-Tech Reports
NOAA/ERL
320 S. Broadway
Boulder, CO 80302

National Center for Atmos Research
NCAR Library
PO Box 3000
Boulder, CO 80307

R. B. Girardo
Bureau of Reclamation
E&R Center, Code 1220
Denver Federal Center, Bldg 67
Denver, CO 80225

National Weather Service
National Meteorological Center
W321, WWB, Room 201
ATTN: Mr. Quiroz
Washington, DC 20233

Mil Assistant for Atmos Sciences
Ofc of the Undersecretary of Defense
for Rsch & Engr/E&LS - Room 3D129
The Pentagon
Washington, DC 20301

Defense Communications Agency
Technical Library Center
Code 205
Washington, DC 20305

Director
Defense Nuclear Agency
ATTN: Technical Library
Washington, DC 20305

HQDA (DAEN-RDM/Dr. de Percin)
Washington, DC 20314

Director
Naval Research Laboratory
Code 5530
Washington, DC 20375

Commanding Officer
Naval Research Laboratory
Code 2627
Washington, DC 20375

Dr. J. M. MacCallum
Naval Research Laboratory
Code 1409
Washington, DC 20375

The Library of Congress
ATTN: Exchange & Gift Div
Washington, DC 20540
2

Head, Atmos Rsch Section
Div Atmospheric Science
National Science Foundation
1800 G. Street, NW
Washington, DC 20550

CPT Hugh Albers, Exec Sec
Interdept Committee on Atmos Science
National Science Foundation
Washington, DC 20550

Director, Systems R&D Service
Federal Aviation Administration
ATTN: ARD-54
2100 Second Street, SW
Washington, DC 20590

ADTC/DLODL
Eglin AFB, FL 32542

Naval Training Equipment Center
ATTN: Technical Library
Orlando, FL 32813

Det 11, 2WS/OI
ATTN: Maj Orondorff
Patrick AFB, FL 32925

USAFETAC/CB
Scott AFB, IL 62225

HQ, ESD/TOSI/S-22
Hanscom AFB, MA 01731

Air Force Geophysics Laboratory
ATTN: LCB (A. S. Carten, Jr.)
Hanscom AFB, MA 01731

Air Force Geophysics Laboratory
ATTN: LYD
Hanscom AFB, MA 01731

Meteorology Division
AFGL/LY
Hanscom AFB, MA 01731

US Army Liaison Office
MIT-Lincoln Lab, Library A-082
PO Box 73
Lexington, MA 02173

Director
US Army Ballistic Rsch Lab
ATTN: DRDAR-BLB (Dr. G. E. Keller)
Aberdeen Proving Ground, MD 21005

Commander
US Army Ballistic Rsch Lab
ATTN: DRDAR-BLP
Aberdeen Proving Ground, MD 21005

Director
US Army Armament R&D Command
Chemical Systems Laboratory
ATTN: DRDAR-CLJ-I
Aberdeen Proving Ground, MD 21010

Chief CB Detection & Alarms Div
Chemical Systems Laboratory
ATTN: DRDAR-CLC-CR (H. Tannenbaum)
Aberdeen Proving Ground, MD 21010

Commander
Harry Diamond Laboratories
ATTN: DELHD-CO
2800 Powder Mill Road
Adelphi, MD 20783

Commander
ERADCOM
ATTN: DRDEL-AP
2800 Powder Mill Road
Adelphi, MD 20783
2

Commander
ERADCOM
ATTN: DRDEL-CG/DRDEL-DC/DRDEL-CS
2800 Powder Mill Road
Adelphi, MD 20783

Commander
ERADCOM
ATTN: DRDEL-CT
2800 Powder Mill Road
Adelphi, MD 20783

Commander
ERADCOM
ATTN: DRDEL-EA
2800 Powder Mill Road
Adelphi, MD 20783

Commander
ERADCOM
ATTN: DRDEL-PA/DRDEL-ILS/DRDEL-E
2800 Powder Mill Road
Adelphi, MD 20783

Commander
ERADCOM
ATTN: DRDEL-PAO (S. Kimmel)
2800 Powder Mill Road
Adelphi, MD 20783

Chief
Intelligence Materiel Dev & Support Ofc
ATTN: DELEW-WL-I
Bldg 4554
Fort George G. Meade, MD 20755

Acquisitions Section, IRDB-D823
Library & Info Service Div, NOAA
6009 Executive Blvd
Rockville, MD 20852

Naval Surface Weapons Center
White Oak Library
Silver Spring, MD 20910

The Environmental Research
Institute of MI
ATTN: IRIA Library
PO Box 8618
Ann Arbor, MI 48107

Mr. William A. Main
USDA Forest Service
1407 S. Harrison Road
East Lansing, MI 48823

Dr. A. D. Belmont
Research Division
PO Box 1249
Control Data Corp
Minneapolis, MN 55440

Director
Naval Oceanography & Meteorology
NSTL Station
Bay St Louis, MS 39529

Director
US Army Engr Waterways Experiment Sta
ATTN: Library
PO Box 631
Vicksburg, MS 39180

Environmental Protection Agency
Meteorology Laboratory
Research Triangle Park, NC 27711

US Army Research Office
ATTN: DRXRO-PP
PO Box 12211
Research Triangle Park, NC 27709

Commanding Officer
US Army Armament R&D Command
ATTN: DRDAR-TSS Bldg 59
Dover, NJ 07801

Commander
HQ, US Army Avionics R&D Activity
ATTN: DAVAA-O
Fort Monmouth, NJ 07703

Commander/Director
US Army Combat Surveillance & Target
Acquisition Laboratory
ATTN: DELCS-D
Fort Monmouth, NJ 07703

Commander
US Army Electronics R&D Command
ATTN: DELCS-S
Fort Monmouth, NJ 07703

US Army Materiel Systems
Analysis Activity
ATTN: DRXSY-MP
Aberdeen Proving Ground, MD 21005

Director
US Army Electronics Technology &
Devices Laboratory
ATTN: DELET-D
Fort Monmouth, NJ 07703

Commander
US Army Electronic Warfare Laboratory
ATTN: DELEW-D
Fort Monmouth, NJ 07703

Commander
US Army Night Vision &
Electro-Optics Laboratory
ATTN: DELNV-L (Dr. Rudolf Buser)
Fort Monmouth, NJ 07703

Commander
ERADCOM Technical Support Activity
ATTN: DELSD-L
Fort Monmouth, NJ 07703

Project Manager, FIREFINDER
ATTN: DRCPM-FF
Fort Monmouth, NJ 07703

Project Manager, REMBASS
ATTN: DRCPM-RBS
Fort Monmouth, NJ 07703

Commander
US Army Satellite Comm Agency
ATTN: DRCPM-SC-3
Fort Monmouth, NJ 07703

Commander
ERADCOM Scientific Advisor
ATTN: DRDEL-SA
Fort Monmouth, NJ 07703

6585 TG/WE
Holloman AFB, NM 88330

AFWL/WE
Kirtland, AFB, NM 87117

AFWL/Technical Library (SUL)
Kirtland AFB, NM 87117

Commander
US Army Test & Evaluation Command
ATTN: STEWS-AD-L
White Sands Missile Range, NM 88002

Rome Air Development Center
ATTN: Documents Library
TSLD (Bette Smith)
Griffiss AFB, NY 13441

Commander
US Army Tropic Test Center
ATTN: STETC-TD (Info Center)
APO New York 09827

Commandant
US Army Field Artillery School
ATTN: ATSF-CD-R (Mr. Farmer)
Fort Sill, OK 73503

Commandant
US Army Field Artillery School
ATTN: ATSF-CF-R
Fort Sill, OK 73503

Director CFD
US Army Field Artillery School
ATTN: Met Division
Fort Sill, OK 73503

Commandant
US Army Field Artillery School
ATTN: Morris Swett Library
Fort Sill, OK 73503

Commander
US Army Dugway Proving Ground
ATTN: MT-DA-L
Dugway, UT 84022

Dr. C. R. Sreedrahan
Research Associates
Utah State University, UNC 48
Logan, UT 84322

Inge Dirmhirn, Professor
Utah State University, UNC 48
Logan, UT 84322

Defense Documentation Center
ATTN: DDC-TCA
Cameron Station Bldg 5
Alexandria, VA 22314
12

Commanding Officer
US Army Foreign Sci & Tech Center
ATTN: DRXST-IS1
220 7th Street, NE
Charlottesville, VA 22901

Naval Surface Weapons Center
Code G65
Dahlgren, VA 22448

Commander
US Army Night Vision
& Electro-Optics Lab
ATTN: DELNV-D
Fort Belvoir, VA 22060

Commander and Director
US Army Engineer Topographic Lab
ETL-TD-MB
Fort Belvoir, VA 22060

Director
Applied Technology Lab
DAVDL-EU-TSD
ATTN: Technical Library
Fort Eustis, VA 23604

Department of the Air Force
OL-C, 5WW
Fort Monroe, VA 23651

Department of the Air Force
5WW/DN
Langley AFB, VA 23665

Director
Development Center MCDEC
ATTN: Firepower Division
Quantico, VA 22134

US Army Nuclear & Chemical Agency
ATTN: MONA-WE
Springfield, VA 22150

Director
US Army Signals Warfare Laboratory
ATTN: DELSW-OS (Dr. R. Burkhardt)
Vint Hill Farms Station
Warrenton, VA 22186

Commander
US Army Cold Regions Test Center
ATTN: STECR-OP-PM
APO Seattle, WA 98733

Dr. John L. Walsh
Code 5560
Navy Research Lab
Washington, DC 20375

Commander
TRASANA
ATTN: ATAA-PL
(Dolores Anguiano)
White Sands Missile Range, NM 88002

Commander
US Army Dugway Proving Ground
ATTN: STEDP-MT-DA-M (Mr. Paul Carlson)
Dugway, UT 84022

Commander
US Army Dugway Proving Ground
ATTN: STEDP-MT-DA-T
(Mr. William Peterson)
Dugway, UT 84022

Commander
USATRADOC
ATTN: ATCD-SIE
Fort Monroe, VA 23651

Commander
USATRADOC
ATTN: ATCD-CF
Fort Monroe, VA 23651

Commander
USATRADOC
ATTN: Tech Library
Fort Monroe, VA 23651

ATMOSPHERIC SCIENCES RESEARCH PAPERS

1. Lindberg, J.D., "An Improvement to a Method for Measuring the Absorption Coefficient of Atmospheric Dust and other Strongly Absorbing Powders, " ECOM-5565, July 1975.
2. Avara, Elton, P., "Mesoscale Wind Shears Derived from Thermal Winds," ECOM-5566, July 1975.
3. Gomez, Richard B., and Joseph H. Pierluissi, "Incomplete Gamma Function Approximation for King's Strong-Line Transmittance Model," ECOM-5567, July 1975.
4. Blanco, A.J., and B.F. Engebos, "Ballistic Wind Weighting Functions for Tank Projectiles," ECOM-5568, August 1975.
5. Taylor, Fredrick J., Jack Smith, and Thomas H. Pries, "Crosswind Measurements through Pattern Recognition Techniques," ECOM-5569, July 1975.
6. Walters, D.L., "Crosswind Weighting Functions for Direct-Fire Projectiles," ECOM-5570, August 1975.
7. Duncan, Louis D., "An Improved Algorithm for the Iterated Minimal Information Solution for Remote Sounding of Temperature," ECOM-5571, August 1975.
8. Robbiani, Raymond L., "Tactical Field Demonstration of Mobile Weather Radar Set AN/TPS-41 at Fort Rucker, Alabama," ECOM-5572, August 1975.
9. Miers, B., G. Blackman, D. Langer, and N. Lorimier, "Analysis of SMS/GOES Film Data," ECOM-5573, September 1975.
10. Manquero, Carlos, Louis Duncan, and Rufus Bruce, "An Indication from Satellite Measurements of Atmospheric CO2 Variability," ECOM-5574, September 1975.
11. Petracca, Carmine, and James D. Lindberg, "Installation and Operation of an Atmospheric Particulate Collector," ECOM-5575, September 1975.
12. Avara, Elton P., and George Alexander, "Empirical Investigation of Three Iterative Methods for Inverting the Radiative Transfer Equation," ECOM-5576, October 1975.
13. Alexander, George D., "A Digital Data Acquisition Interface for the SMS Direct Readout Ground Station — Concept and Preliminary Design," ECOM-5577, October 1975.
14. Cantor, Israel, "Enhancement of Point Source Thermal Radiation Under Clouds in a Nonattenuating Medium," ECOM-5578, October 1975.
15. Norton, Colburn, and Glenn Hoidale, "The Diurnal Variation of Mixing Height by Month over White Sands Missile Range, N.M," ECOM-5579, November 1975.
16. Avara, Elton P., "On the Spectrum Analysis of Binary Data," ECOM-5580, November 1975.
17. Taylor, Fredrick J., Thomas H. Pries, and Chao-Huan Huang, "Optimal Wind Velocity Estimation," ECOM-5581, December 1975.
18. Avara, Elton P., "Some Effects of Autocorrelated and Cross-Correlated Noise on the Analysis of Variance, " ECOM-5582, December 1975.
19. Gillespie, Patti S., R.L. Armstrong, and Kenneth O. White, "The Spectral Characteristics and Atmospheric CO2 Absorption of the Ho^{+3}:YLF Laser at 2.05μm," ECOM-5583, December 1975.
20. Novlan, David J. "An Empirical Method of Forecasting Thunderstorms for the White Sands Missile Range," ECOM-5584, February 1976.
21. Avara, Elton P., "Randomization Effects in Hypothesis Testing with Autocorrelated Noise," ECOM-5585, February 1976.
22. Watkins, Wendell R., "Improvements in Long Path Absorption Cell Measurement," ECOM-5586, March 1976.
23. Thomas, Joe, George D. Alexander, and Marvin Dubbin, "SATTEL — An Army Dedicated Meteorological Telemetry System," ECOM-5587. March 1976.
24. Kennedy, Bruce W., and Delbert Bynum, "Army User Test Program for the RDT&E-XM-75 Meteorological Rocket," ECOM-5588, April 1976.

25. Barnett, Kenneth M., "A Description of the Artillery Meteorological Comparisons at White Sands Missle Range, October 1974 - December 1974 ('PASS' - Prototype Artillery [Meteorological] Subsystem)," ECOM-5589, April 1976.
26. Miller, Walter B., "Preliminary Analysis of Fall-of-Shot From Project 'PASS'," ECOM-5590, April 1976.
27. Avara, Elton P., "Error Analysis of Minimum Information and Smith's Direct Methods for Inverting the Radiative Transfer Equation," ECOM-5591, April 1976.
28. Yee, Young P., James D. Horn, and George Alexander, "Synoptic Thermal Wind Calculations from Radiosonde Observations Over the Southwestern United States," ECOM-5592, May 1976.
29. Duncan, Louis D., and Mary Ann Seagraves, "Applications of Empirical Corrections to NOAA-4 VTPR Observations," ECOM-5593, May 1976.
30. Miers, Bruce T., and Steve Weaver, "Applications of Meterological Satellite Data to Weather Sensitive Army Operations,"ECOM-5594, May 1976.
31. Sharenow, Moses, "Redesign and Improvement of Balloon ML-566," ECOM-5595, June, 1976.
32. Hansen, Frank V., "The Depth of the Surface Boundary Layer," ECOM-5596, June 1976.
33. Pinnick, R.G., and E.B. Stenmark, "Response Calculations for a Commercial Light-Scattering Aerosol Counter," ECOM-5597, July 1976.
34. Mason, J., and G.B. Hoidale, "Visibility as an Estimator of Infrared Transmittance," ECOM-5598, July 1976.
35. Bruce, Rufus E., Louis D. Duncan, and Joseph H. Pierluissi, "Experimental Study of the Relationship Between Radiosonde Temperatures and Radiometric-Area Temperatures," ECOM-5599, August 1976.
36. Duncan, Louis D., "Stratospheric Wind Shear Computed from Satellite Thermal Sounder Measurements," ECOM-5800, September 1976.
37. Taylor, F., P. Mohan, P. Joseph and T. Pries, "An All Digital Automated Wind Measurement System," ECOM-5801, September 1976.
38. Bruce, Charles, "Development of Spectrophones for CW and Pulsed Radiation Sources," ECOM-5802, September 1976.
39. Duncan, Louis D., and Mary Ann Seagraves,"Another Method for Estimating Clear Column Radiances," ECOM-5803, October 1976.
40. Blanco, Abel J., and Larry E. Taylor, "Artillery Meteorological Analysis of Project Pass," ECOM-5804, October 1976.
41. Miller, Walter, and Bernard Engebos," A Mathematical Structure for Refinement of Sound Ranging Estimates," ECOM-5805, November, 1976.
42. Gillespie, James B., and James D. Lindberg, "A Method to Obtain Diffuse Reflectance Measurements from 1.0 to 3.0 μm Using a Cary 17I Spectrophotometer," ECOM-5806, November 1976.
43. Rubio, Roberto, and Robert O. Olsen,"A Study of the Effects of Temperature Variations on Radio Wave Absorption,"ECOM-5807, November 1976.
44. Ballard, Harold N., "Temperature Measurements in the Stratosphere from Balloon-Borne Instrument Platforms, 1968-1975," ECOM-5808, December 1976.
45. Monahan, H.H., "An Approach to the Short-Range Prediction of Early Morning Radiation Fog," ECOM-5809, January 1977.
46. Engebos, Bernard Francis, "Introduction to Multiple State Multiple Action Decision Theory and Its Relation to Mixing Structures," ECOM-5810, January 1977.
47. Low, Richard D.H.,"Effects of Cloud Particles on Remote Sensing from Space in the 10-Micrometer Infrared Region," ECOM-5811, January 1977.
48. Bonner, Robert S., and R. Newton, "Application of the AN/GVS-5 Laser Rangefinder to Cloud Base Height Measurements," ECOM-5812, February 1977.
49. Rubio, Roberto, "Lidar Detection of Subvisible Reentry Vehicle Erosive Atmospheric Material," ECOM-5813, March 1977.
50. Low, Richard D.H., and J.D. Horn, "Mesoscale Determination of Cloud-Top Height: Problems and Solutions," ECOM-5814, March 1977.

51. Duncan, Louis D., and Mary Ann Seagraves,"Evaluation of the NOAA-4 VTPR Thermal Winds for Nuclear Fallout Predictions," ECOM-5815, March 1977.
52. Randhawa, Jagir S., M. Izquierdo, Carlos McDonald and Zvi Salpeter, "Stratospheric Ozone Density as Measured by a Chemiluminescent Sensor During the Stratcom VI-A Flight," ECOM-5816, April 1977.
53. Rubio, Roberto, and Mike Izquierdo, "Measurements of Net Atmospheric Irradiance in the 0.7- to 2.8-Micrometer Infrared Region," ECOM-5817, May 1977.
54. Ballard, Harold N., Jose M. Serna, and Frank P. Hudson Consultant for Chemical Kinetics, "Calculation of Selected Atmospheric Composition Parameters for the Mid-Latitude, September Stratosphere," ECOM-5818, May 1977.
55. Mitchell, J.D., R.S. Sagar, and R.O. Olsen, "Positive Ions in the Middle Atmosphere During Sunrise Conditions," ECOM-5819, May 1977.
56. White, Kenneth O., Wendell R. Watkins, Stuart A. Schleusener, and Ronald L. Johnson, "Solid-State Laser Wavelength Identification Using a Reference Absorber," ECOM-5820, June 1977.
57. Watkins, Wendell R., and Richard G. Dixon, "Automation of Long-Path Absorption Cell Measurements," ECOM-5821, June 1977.
58. Taylor, S.E., J.M. Davis, and J.B. Mason, "Analysis of Observed Soil Skin Moisture Effects on Reflectance," ECOM-5822, June 1977.
59. Duncan, Louis D. and Mary Ann Seagraves, "Fallout Predictions Computed from Satellite Derived Winds," ECOM-5823. June 1977.
60. Snider, D.E., D.G. Murcray, F.H. Murcray, and W.J. Williams, "Investigation of High-Altitude Enhanced Infrared Backround Emissions" (U), SECRET, ECOM-5824, June 1977.
61. Dubbin, Marvin H. and Dennis Hall, "Synchronous Meteorlogical Satellite Direct Readout Ground System Digital Video Electronics," ECOM-5825, June 1977.
62. Miller, W., and B. Engebos, "A Preliminary Analysis of Two Sound Ranging Algorithms," ECOM-5826, July 1977.
63. Kennedy, Bruce W., and James K. Luers, "Ballistic Sphere Techniques for Measuring Atomspheric Parameters," ECOM-5827, July 1977.
64. Duncan, Louis D., "Zenith Angle Variation of Satellite Thermal Sounder Measurements," ECOM-5828, August 1977.
65. Hansen, Frank V., "The Critical Richardson Number," ECOM-5829, September 1977.
66. Ballard, Harold N., and Frank P. Hudson (Compilers), "Stratospheric Composition Balloon-Borne Experiment," ECOM-5830, October 1977.
67. Barr, William C., and Arnold C. Peterson, "Wind Measuring Accuracy Test of Meteorological Systems," ECOM-5831, November 1977.
68. Ethridge, G.A. and F.V. Hansen, "Atmospheric Diffusion: Similarity Theory and Empirical Derivations for Use in Boundary Layer Diffusion Problems," ECOM-5832, November 1977.
69. Low, Richard D.H., "The Internal Cloud Radiation Field and a Technique for Determining Cloud Blackness," ECOM-5833, December 1977.
70. Watkins, Wendell R., Kenneth O. White, Charles W. Bruce, Donald L. Walters, and James D. Lindberg, "Measurements Required for Prediction of High Energy Laser Transmission," ECOM-5834, December 1977.
71. Rubio, Robert, "Investigation of Abrupt Decreases in Atmospherically Backscattered Laser Energy," ECOM-5835. December 1977.
72. Monahan, H.H. and R.M. Cionco, "An Interpretative Review of Existing Capabilities for Measuring and Forecasting Selected Weather Variables (Emphasizing Remote Means)," ASL-TR-0001, January 1978.
73. Heaps, Melvin G., "The 1979 Solar Eclipse and Validation of D-Region Models," ASL-TR-0002. March 1978.

74. Jennings, S.G., and J.B. Gillespie, "M.I.E. Theory Sensitivity Studies - The Effects of Aerosol Complex Refractive Index and Size Distribution Variations on Extinction and Absorption Coefficients Part II: Analysis of the Computational Results," ASL-TR-0003, March 1978.
75. White, Kenneth O. et al, "Water Vapor Continuum Absorption in the 3.5μm to 4.0μm Region," ASL-TR-0004, March 1978.
76. Olsen, Robert O., and Bruce W. Kennedy, "ABRES Pretest Atmospheric Measurements," ASL-TR-0005, April 1978.
77. Ballard, Harold N., Jose M. Serna, and Frank P. Hudson, "Calculation of Atmospheric Composition in the High Latitude September Stratosphere," ASL-TR-0006, May 1978.
78. Watkins, Wendell R. et al, "Water Vapor Absorption Coefficients at HF Laser Wavelengths," ASL-TR-0007, May 1978.
79. Hansen, Frank V., "The Growth and Prediction of Nocturnal Inversions," ASL-TR-0008, May 1978.
80. Samuel, Christine, Charles Bruce, and Ralph Brewer, "Spectrophone Analysis of Gas Samples Obtained at Field Site," ASL-TR-0009, June 1978.
81. Pinnick, R.G. et al., "Vertical Structure in Atmospheric Fog and Haze and its Effects on IR Extinction," ASL-TR-0010, July 1978.
82. Low, Richard D.H., Louis D. Duncan, and Richard B. Gomez, "The Microphysical Basis of Fog Optical Characterization," ASL-TR-0011, August 1978.
83. Heaps, Melvin G., "The Effect of a Solar Proton Event on the Minor Neutral Constituents of the Summer Polar Mesosphere," ASL-TR-0012, August 1978.
84. Mason, James B., "Light Attenuation in Falling Snow," ASL-TR-0013, August 1978.
85. Blanco, Abel J., "Long-Range Artillery Sound Ranging: "PASS" Meteorological Application," ASL-TR-0014, September 1978.
86. Heaps, M.G., and F.E. Niles, "Modeling the Ion Chemistry of the D-Region: A case Study Based Upon the 1966 Total Solar Eclipse," ASL-TR-0015, September 1978.
87. Jennings, S.G., and R.G. Pinnick, "Effects of Particulate Complex Refractive Index and Particle Size Distribution Variations on Atmospheric Extinction and Absorption for Visible Through Middle-Infrared Wavelengths," ASL-TR-0016, September 1978.
88. Watkins, Wendell R., Kenneth O. White, Lanny R. Bower, and Brian Z. Sojka, " Pressure Dependence of the Water Vapor Continuum Absorption in the 3.5- to 4.0-Micrometer Region," ASL-TR-0017, September 1978.
89. Miller, W.B., and B.F. Engebos, "Behavior of Four Sound Ranging Techniques in an Idealized Physical Enviroment," ASL-TR-0018, September 1978.
90. Gomez, Richard G., "Effectiveness Studies of the CBU-88/B Bomb, Cluster, Smoke Weapon" (U), CONFIDENTIAL ASL-TR-0019, September 1978.
91. Miller, August, Richard C. Shirkey, and Mary Ann Seagraves, "Calculation of Thermal Emission from Aerosols Using the Doubling Technique," ASL-TR-0020, November, 1978.
92. Lindberg, James D. et al., "Measured Effects of Battlefield Dust and Smoke on Visible, Infrared, and Millimeter Wavelengths Propagation: A Preliminary Report on Dusty Infrared Test-I (DIRT-I)," ASL-TR-0021, January 1979.
93. Kennedy, Bruce W., Arthur Kinghorn, and B.R. Hixon, "Engineering Flight Tests of Range Meteorological Sounding System Radiosonde," ASL-TR-0022, February 1979.
94. Rubio, Roberto, and Don Hoock, "Microwave Effective Earth Radius Factor Variability at Wiesbaden and Balboa," ASL-TR-0023, February 1979.
95. Low, Richard D.H., "A Theoretical Investigation of Cloud/Fog Optical Properties and Their Spectral Correlations," ASL-TR-0024, February 1979.

96. Pinnick, R.G., and H.J. Auvermann, "Response Characteristics of Knollenberg Light-Scattering Aerosol Counters," ASL-TR-0025, February 1979.
97. Heaps, Melvin G., Robert O. Olsen, and Warren W. Berning, "Solar Eclipse 1979, Atmospheric Sciences Laboratory Program Overview," ASL-TR-0026 February 1979.
98. Blanco, Abel J., "Long-Range Artillery Sound Ranging: 'PASS' GR-8 Sound Ranging Data," ASL-TR-0027, March 1979.
99. Kennedy, Bruce W., and Jose M. Serna, "Meteorological Rocket Network System Reliability," ASL-TR-0028, March 1979.
100. Swingle, Donald M., "Effects of Arrival Time Errors in Weighted Range Equation Solutions for Linear Base Sound Ranging," ASL-TR-0029, April 1979.
101. Umstead, Robert K., Ricardo Pena, and Frank V. Hansen, "KWIK: An Algorithm for Calculating Munition Expenditures for Smoke Screening/Obscuration in Tactical Situations," ASL-TR-0030, April 1979.
102. D'Arcy, Edward M., "Accuracy Validation of the Modified Nike Hercules Radar," ASL-TR-0031, May 1979.
103. Rodriguez, Ruben, "Evaluation of the Passive Remote Crosswind Sensor," ASL-TR-0032, May 1979.
104. Barber, T.L., and R. Rodriguez, "Transit Time Lidar Measurement of Near-Surface Winds in the Atmosphere," ASL-TR-0033, May 1979.
105. Low, Richard D.H., Louis D. Duncan, and Y.Y. Roger R. Hsiao, "Microphysical and Optical Properties of California Coastal Fogs at Fort Ord," ASL-TR-0034, June 1979.
106. Rodriguez, Ruben, and William J. Vechione, "Evaluation of the Saturation Resistant Crosswind Sensor," ASL-TR-0035, July 1979
107. Ohmstede, William D., "The Dynamics of Material Layers," ASL-TR-0036, July 1979.
108. Pinnick, R.G., S.G. Jennings, Petr Chýlek, and H.J. Auvermann "Relationships between IR Extinction, Absorption, and Liquid Water Content of Fogs," ASL-TR-0037, August 1979
109. Rodriguez, Ruben, and William J. Vechione, "Performance Evaluation of the Optical Crosswind Profiler," ASL-TR-0038, August 1979
110. Miers, Bruce T., "Precipitation Estimation Using Satellite Data" ASL-TR-0039, September 1979
111. Dickson, David H., and Charles M. Sonnenschein, "Helicopter Remote Wind Sensor System Description," ASL-TR-0040, September 1979
112. Heaps, Melvin G., and Joseph M. Heimerl, "Validation of the Dairchem Code, I: Quiet Midlatitude Conditions," ASL-TR-0041, September 1979

☆ U.S. GOVERNMENT PRINTING OFFICE: 1979 — 677-119/38